

Mechanical response of the flux lines in ceramic $\text{YBa}_2\text{Cu}_3\text{O}_{7-\delta}$

J. Luzuriaga,* M.-O. André, and W. Benoit

Institut de Genie Atomique, Ecole Polytechnique Federal de Lausanne, (1015) Ecublens, Switzerland

(Received 26 December 1991)

We have studied the mechanical response of the flux-line lattice (FLL) in ceramic samples of $\text{YBa}_2\text{Cu}_3\text{O}_7$ by means of a low-frequency forced pendulum. The internal friction and elastic modulus variation of the FLL have been measured as a function of temperature for different values of the applied stress. A somewhat different behavior was observed whether a zero-field-cooling or field-cooling procedure was followed. Measurements of the internal friction and elastic modulus as a function of the applied stress at constant temperature show amplitude-dependent dissipation, with a maximum dissipation at intermediate values of the stress. This dependence is well fitted by a rheological model of extended dry friction, if we restrict ourselves to the dissipation and modulus at fixed temperature. The agreement is not so good when attempting to extend the model to fit the temperature dependence.

I. INTRODUCTION

Because of the great importance of flux pinning for achieving useful values of the critical current in type-II superconductors, there has been continuing interest in investigating the vortex-pinning center interactions, as well as the collective properties of the vortex assembly.

The behavior of the flux-line lattice (FLL) in superconductors has been studied traditionally by measuring the magnetization, the susceptibility, or the critical current (e.g., by the four-probe technique). More recently, the measurement of the mechanical response of the vortices has allowed a way of probing the coupling of the vortex lattice to the pinning centers in superconducting materials. There exist several ways of measuring the mechanical response of the vortices, and they can be grouped for convenience according to the frequency at which they operate.

The first to be developed were audio-frequency measurements using vibrating reeds¹ and high- Q mechanical oscillators.² This technique involves measuring the resonance frequency and dissipation in an oscillator made of a superconductor, or which has a superconductor attached, when the material is in the vortex state. The vortices exert an extra restoring force and dissipate energy because of their interaction with the magnetic field, and for small displacements from their equilibrium position, a theory developed by Brandt, and co-workers¹ permits one to relate the measured resonance frequency and dissipation to parameters of the FLL, for the case of the vibrating reed. However, this theory should not apply if the relative displacement of vortices and pinning centers becomes comparable to the maximum displacement of the reed, which is between 100 and 4000 nm in most experiments. Also in the same frequency domain is the vibrating-bar system of Baar and Harrison.^{3,4} This frequency range is perhaps the most widely explored.¹⁻¹¹

Experiments on ultrasound propagation when the sample is in the vortex state,¹²⁻¹⁴ probe the vortex-defect interactions at megahertz frequencies. In these exper-

iments the amplitude of the relative displacements of the vortex and pinning centers is probably the lowest one achieved in any of the mechanical measurements described here (10 nm as an upper limit¹³).

The low-frequency domain is explored by torsional pendulums,¹⁵⁻¹⁸ which cover the range between fractions of a millihertz and a few hertz. Here the displacements at the tip of the sample are between 250 and 5000 nm. However, in this case the sample is rotated about an axis, so one should consider the deflection angle as more important.

In some of the above methods, i.e., a vibrating reed made of the same material which pins the vortices or ultrasound propagation, there is a deformation of the sample, while in others, the superconducting material remains undeformed. The results seem to be the same, however, whether there is deformation or not, although a more stringent test, such as measuring the same sample with and without deformation remains to be performed.

A feature common to all the measurements of the mechanical coupling between vortices and high- T_c superconducting materials is that a peak in the dissipation and a corresponding decrease in the stiffness of the FLL is seen well below T_c when the temperature is swept at constant magnetic field. The peak appears at reduced temperatures $t = T/T_c$, which although sample dependent are typically $t \simeq 0.4$ in $\text{Bi}_2\text{Sr}_2\text{CaCu}_2\text{O}_8$, $t \simeq 0.7$ in $\text{La}_{1.8}\text{Sr}_{0.2}\text{CuO}_4$, and $t \simeq 0.95$ in $\text{YBa}_2\text{Cu}_3\text{O}_{7-\delta}$. There is currently a controversy as to the origin of this feature. While some authors consider it to be evidence for flux lattice melting^{2,19-22} or some transition to a glassy state of the flux structure,⁵ others interpret the measurements in terms of thermal activation^{10,23} akin to the "giant flux creep"^{24,25} or thermally activated flux flow²⁶ (TAFF) explanations given in the closely related situations of flux creep and reversibility line measurements.

In this paper, we present results of low-frequency measurements of the mechanical response of the FLL in ceramic YBCO, in particular of the behavior as a function of the stress applied to the vortex lattice. We find that

the dissipation and stiffness of the FLL depend on the stress, and that a temperature-dependent critical stress can be defined. A rheological model, proposing an extended dry friction mechanism, partially fits the experimental observations.

II. EXPERIMENTAL DETAILS

Measurements have been carried out in ceramic samples of $\text{YBa}_2\text{Cu}_3\text{O}_{7-\delta}$, prepared from commercial powders of the compound, which were pressed at 2000 kg/cm^3 for 15 min and subsequently heated to a temperature of $940 \text{ }^\circ\text{C}$ for 50 h in a pure oxygen atmosphere. The density of the resultant ceramic was around 5.1 g/cm^3 . Sample dimensions were $50 \times 10 \times 1 \text{ mm}^3$ and the slabs were cut from the original pellet with a diamond saw. The resistive transition has its midpoint at around 85 K with a $\sim 1.5 \text{ K}$ width and is shown in the inset of Fig. 5.

The torsional pendulum rotates in a vertical axis,¹⁵ and the magnetic field is in the horizontal direction. When there are pinned vortices in the sample a restoring force of magnetic origin appears, in a way similar to what happens in the vibrating reed,¹ and this is added to the torque provided by the suspension wire. With the present configuration and for a magnetic field of 0.08 T, the magnetic restoring torque of the FLL is around 25% of that of the suspension wire, which is a tungsten filament of 5 mm length and 0.3 mm diameter. The pendulum is forced to oscillate at low frequencies, below its resonance frequency, which in our case, due to the relatively weak restoring torque, was of about 10 Hz. Thus the measurements can extend from around a millihertz to around 5 Hz, where the effects of the resonance start to become too important. In the present apparatus, the torsional modulus is measured through the change in the amplitude of the response when a constant force is applied to the pendulum, and the attenuation is obtained by measuring the phase lag between signal and response.¹⁶ The suspension wire remains at constant temperature, so it contributes a constant background in temperature sweeps. The sample is not deformed when the pendulum rotates, and the vortices can be regarded as forced to tilt, but not to bend, during the measurement.

III. EXPERIMENTAL RESULTS

A. Temperature sweeps

In Fig. 1, we show the internal friction (F_i) and change in torsional modulus (G) due to the vortices, as a function of temperature for an applied magnetic field of 0.08 T. In all the measurements the frequency was 1 Hz, and the curves correspond to different values of the applied stress.

Stress is presented in arbitrary units, but it can be related to the associated strain, i.e., the deflection of the sample from its equilibrium position. The restoring torque is given both by the suspension wire and the magnetic contribution, and for a crude estimate we can ignore the $\sim 25\%$ magnetic contribution, so stress and strain are linear. Within this approximation, we have

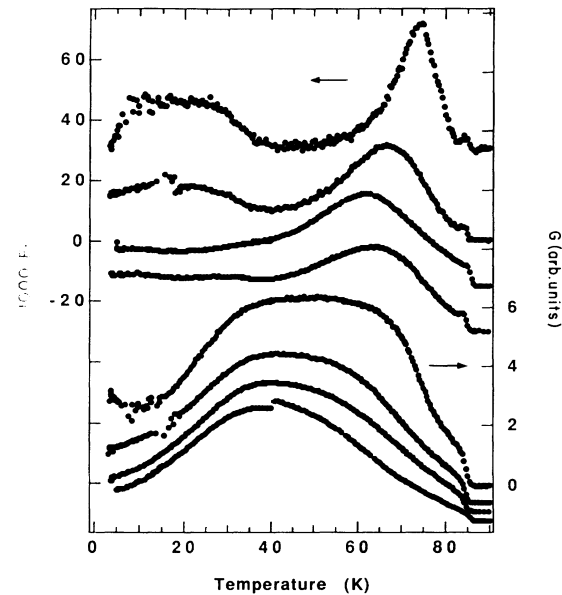


FIG. 1. Results for the stiffness G and internal friction F_i of the FLL on heating at 0.3 K/min after applying a field of 0.08 T at low temperature (ZFC). The curves (which have been displaced in the vertical direction for clarity) correspond to different values of the applied stress (in arbitrary units), corresponding to: 0.01, 0.04, 0.08, and 0.2 from the upper to the lower curves. An arbitrary unit of stress corresponds roughly to a vibration angle of $5 \times 10^{-2} \text{ rad}$.

found that an arbitrary unit of stress produces a deflection of $5 \times 10^{-2} \text{ rad}$ in the pendulum. However, it should be kept in mind that in the experiment the variable which is controlled is the stress.

All the above measurements were done using the zero-field-cooling (ZFC) procedure, that is, the sample was cooled in the remanent field of the apparatus, then the measuring field was applied, and the temperature was increased at around 0.3 K/min , while monitoring $G(T)$ and $F_i(T)$. It can be seen that there is some difference between the F_i curves, the one taken at lower stress showing more structure than the others. For the lower stress curve, the F_i has a small value at 4 K, which increases with increasing temperature, until $\sim 15 \text{ K}$, then there is a plateau between 18 and 28 K approximately, a descent until 40 K, a new plateau at a low value, and then a rather broad peak in the F_i between roughly 65 and 80 K. For curves taken at higher stress, the peak broadens and the structure at low temperatures gradually disappears. The change in the apparent torsional modulus G goes from a low value at low temperatures to a plateau at high temperatures and then a drop between roughly 60 and 80 K. The main difference between the $G(T)$ curves is that the plateau is lower the higher the stress at which the curve was taken. In both the F_i and G measurements, it is possible to see a step in the measured quantity at a temperature corresponding to T_c obtained by measuring the resistance. (See inset of Fig. 5).

Figure 2 also shows data of temperature sweeps at dif-

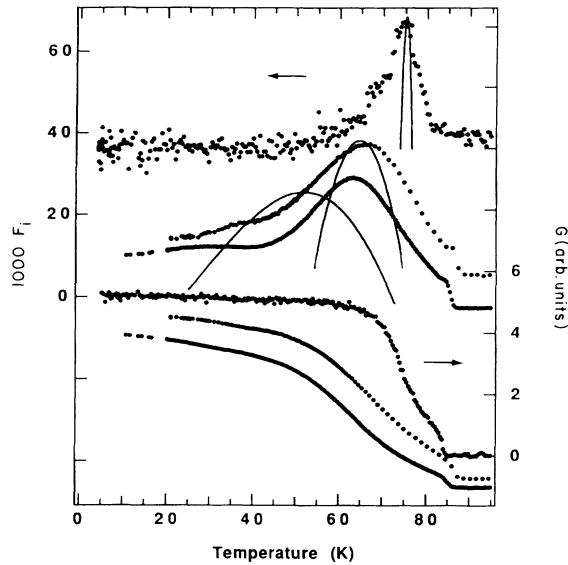


FIG. 2. Field cooling (FC) results under the same conditions as Fig. 1. The applied stress (in arbitrary units) corresponds to: 0.01, 0.08, and 0.2 from the upper to the lower curves. Solid lines are results of a fit to Eqs. (1) and (3) defined in the text. Curves have been shifted in the vertical direction for clarity; they should all coincide above 86 K.

ferent amplitudes but taken with a field-cooling (FC) procedure, that is, the sample was cooled in an applied magnetic field. The field, temperature, and sweep-time rate were the same as for the ZFC case. Two main differences are seen between the FC and ZFC cases. For FC, there is practically no structure at temperatures below the peak in the F_i measurements, and the change in G is monotonous, starting at a high value at low temperatures and then having a steplike descent. The other trends seen in ZFC, such as the broadening of the F_i peak, and its shift to lower temperatures when the curves are taken at higher stress, apply also to the FC case.

B. Amplitude sweeps at constant temperature

We have also performed measurements as a function of the applied stress, maintaining the temperature constant, and the results are shown in Fig. 3. It can be seen that there is a strong dependence of the F_i on the applied stress, that is, the damping is not due to a force linear in the velocity (viscous damping), which gives amplitude-independent dissipation. Nonlinear damping has been seen frequently in vibrating reed studies^{1,7,8} and it is hoped that the present measurements as a function of the applied stress will permit a better characterization of the phenomenon. There is a peak in the F_i as a function of stress, as was seen by D'Anna and co-workers.^{15,16} The maximum is higher when the curve is taken at temperatures which correspond roughly to those where the peak in the F_i -vs- T curves is seen. The peak, however, subsists even in the F_i -vs- σ curves taken at low temperatures, although our measurement range does not allow the full descent of the peak to be seen. There is a qualitative

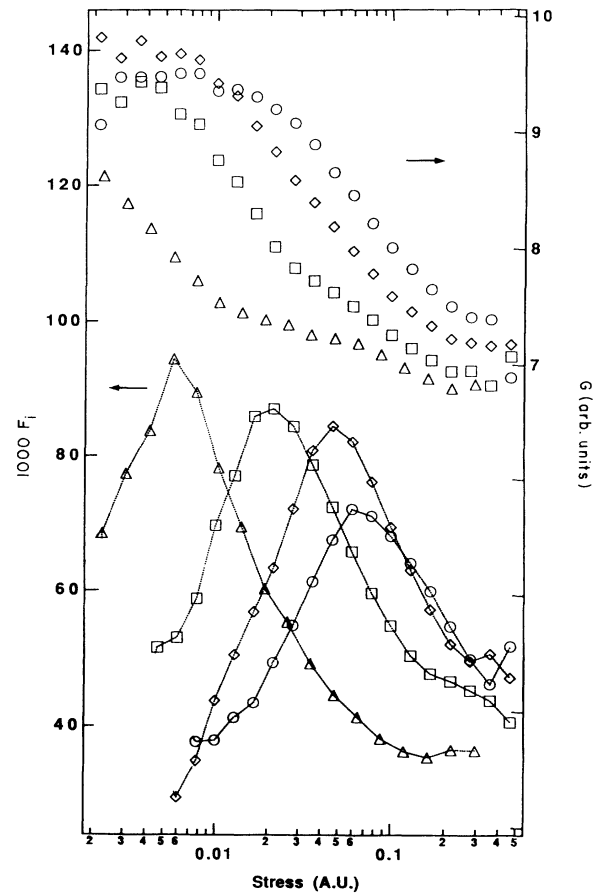


FIG. 3. Stress dependence of F_i and G for different temperatures; Δ , $T = 77$ K; \square , $T = 74$ K; \diamond , $T = 71$ K; \circ , $T = 67.5$ K. The applied field is 0.08 T and the measuring frequency 1 Hz. Lines are only guides for the eye.

change in the shape of the F_i -vs- σ curves measured at lower temperatures; they show a monotonously increasing background superposed to the peak.

IV. DISCUSSION

A. Zero-field-cooling and field-cooling curves

The difference between the ZFC and FC measurements of $G(T)$ and $F_i(T)$ seen in Figs. 1 and 2 can be attributed to the different state of magnetization of the sample after each of the cooling procedures. In particular, considering the ZFC curve taken at lower stress ($\sigma=0.01$) we can interpret the four distinct zones seen in $F_i(T)$ and $G(T)$ as follows: The lowest-temperature zone extends from about 4 to 15 K, and is characterized by an F_i which is increasing in temperature and a fairly stable modulus G . This feature can be explained if we assume that the sample is in a critical state, where the vortices are inhibited from entering the sample by the pinning forces. These forces grow weaker as the temperature is raised, thus increasing the dissipation as vortices move around their equilibrium positions, but they are still strong enough to

stop the vortices from entering and so the stiffness of the lattice is fairly constant, corresponding to a fixed number of vortices. In the second region, for T between ~ 15 and ~ 40 K we can suppose that vortices enter the sample, thus increasing the stiffness $G(T)$ until it saturates when they reach equilibrium, while there is a plateau in the F_i followed later by a descent. In the third region, between ~ 40 and ~ 65 K, $G(T)$ is constant and the F_i is also constant at a relatively low value. This can be interpreted by assuming that the lattice is in a stabler position, closer to equilibrium, and that this denser lattice is more rigidly pinned and thus dissipates less energy. Finally, between 65 and 80 K there is a peak in dissipation and associated decrease in modulus which is also observed in the FC curves and is present in all measurements of mechanical response of the vortices. For curves taken at higher stress, the increase in F_i observed between ~ 4 and ~ 15 K gradually disappears, and it seems that stress-induced depinning drives the vortices to their equilibrium positions and thus shifts the curves towards the shape taken by the corresponding FC curves.

B. Stress dependence

The dependence of the F_i as a function of stress seen in Fig. 3 is markedly different from the more frequent, amplitude-independent, viscous damping observed in measurements of F_i in solids. Viscous damping is usually analyzed in terms of the well-known rheological model of the "standard anelastic solid."²⁷ Amplitude-dependent, hysteretic damping, on the other hand, can be described by a model of "extended dry friction,"²⁸ which is depicted in the inset of Fig. 4. The difference between this model and the standard anelastic solid is that the "dashpot" providing the *viscous* (i.e., proportional to velocity) force has been replaced by a "dry friction" mechanism, which gives a *constant* (velocity-independent) force whenever a critical stress is surpassed and is lossless and rigid if the stress is below critical.

The model predicts an F_i which is zero when the applied stress σ is below the critical stress σ_c and becomes

$$F_i = \Delta \frac{4\sigma_c(\sigma - \sigma_c)}{\pi\sigma^2} \quad (1)$$

when the applied stress is above the critical value. We obtained the critical stress σ_c and maximum attenuation F_{im} from the F_i -vs- σ plots, and normalized the curves by plotting F_i/F_{im} against σ/σ_c . Similarly, we normalized the curves for the decrease in torsional modulus by plotting G vs σ/σ_c . Typical results are shown in Fig. 4 and it can be seen that all curves taken between 65 and 77 K fall on the same universal curve, and that Eq. (1) provides a good fit for the data. The fit is worse at low stress, where the rise is not as steep as expected if a single critical stress exists, but the overall fit is quite good, and some distribution of σ_c could be responsible for the broadening observed at low stress (notice the logarithmic scale, which tends to emphasize the differences by stretching the lower part of the scale).

In Fig. 5 we plot σ_c as a function of the temperature

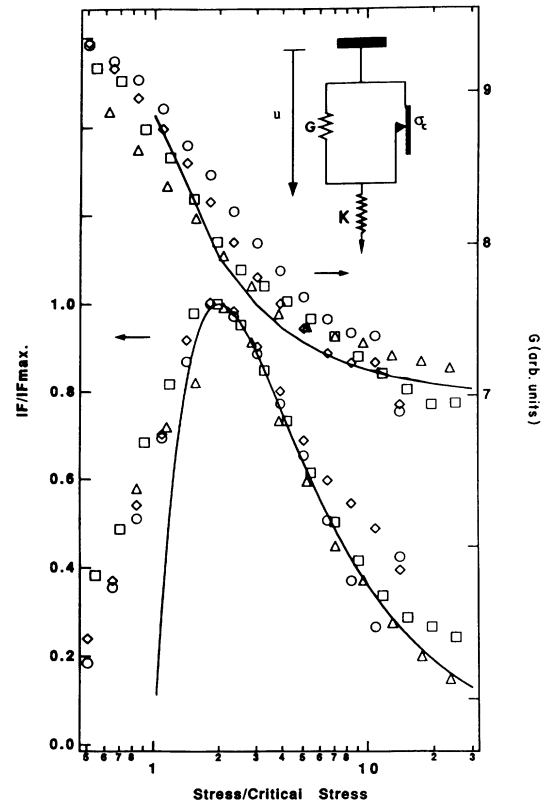


FIG. 4. Same data as in Fig. 3 plotted in normalized units. Solid lines are the calculated values for F_i and G given by the extended dry friction model shown in the inset.

at which the curves were taken, for two values of the applied magnetic field. The data lie in a straight line, which changes slightly depending on the field applied, and the critical stress extrapolates to zero at around 76 or 78 K.

The rheological model which gives Eq. (1) has been applied to the problem of a dislocation moving in a dense cloud of point defects.²⁸ In this case, thermal activation can play a role, and it gives rise to a decrease of the critical stress with temperature. The behavior of a model which assumes the usual form of thermal activation, introducing the Boltzmann factor and considering that the peak in attenuation corresponds to the situation where the jump frequency equals the measurement frequency, produces an equation for the critical stress²⁸ that has the following frequency and temperature dependence:

$$\sigma_c = \sigma_0 \left(1 - \frac{kT}{\Delta F} \ln \frac{2\pi\nu}{\omega} \right)^n, \quad (2)$$

where ΔF is the potential energy to be jumped over, ν is the attack frequency, σ_0 is the critical stress at zero temperature, and n is an exponent which depends on the shape of the pinning potential. It can be seen that the data in Fig. 5 show a linear relationship

$$\sigma_c = \sigma_0 + \alpha T \quad (3)$$

with $\sigma_0=0.264$ (in the arbitrary units used through-

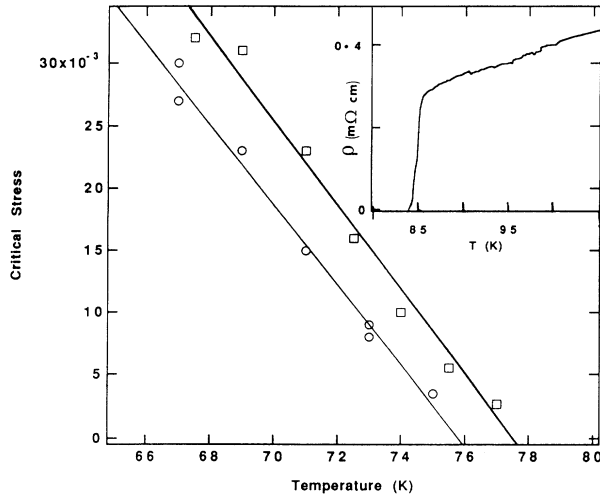


FIG. 5. Critical stress as a function of temperature, as measured from curves of the type shown in Fig. 3. Applied field: $\square = 0.08$ T; $\circ = 0.14$ T. Inset: Resistive transition.

out this paper), $\alpha = 3.42 \times 10^{-3}$ a.u./K and $\sigma_0 = 0.246$, $\alpha = 3.25 \times 10^{-3}$ a.u./K for $H = 0.08$ and 0.14 T, respectively. According to the thermal activation model, however, α should have to be frequency-dependent although with a weak (logarithmic) frequency dependence. Measurements as a function of frequency²⁹ have failed to show the dependence expected if one assumes reasonable values for ν in Eq. (2).

Combining Eqs. (1) and (3), it is possible to derive a formula for the temperature variation of the F_i at a constant applied stress. Now it is the variation in critical stress with temperature that is responsible for the peak, and the consistency of the model can be tested. Results of this type of fits are shown in Fig. 2 as full lines. The height of the peak has been taken from the F_i -vs- σ curves and although its numerical value shows a great dispersion, we have loosely fitted it by a cubic polynomial, since it is not independent of temperature. The temperature variation of σ_c has been taken from Eq. (3) and the fitted parameters, with no further manipulation. It can be seen from the graph that only part of the observed change in F_i is approximated by the equations, because the curves observed are much broader than those calculated. That is not too surprising, however, because it is not too realistic to have a single value of the critical stress for all vortices, but rather a distribution of σ_c .

The position of the calculated peaks seem to be in fair agreement with experiment, at least for the two curves taken at lower stress. The peak of the curve measured at $\sigma = 0.2$ appears at a temperature much higher than calculated, but it must be kept in mind that we are using a value of the applied stress that is outside the range covered by the measurements shown in Fig. 5. We have found that the linear extrapolation of σ_c to lower temperatures does not agree with the measured σ_c ,²⁹ but there seems to be no point in using a more complicated expression than Eq. (3) at the present stage.

V. CONCLUSIONS

The rheological model giving Eq. (1) appears to be a good phenomenological description, as evidenced by the rather good accord between the model and experiment seen in Fig. 4 and the poorer one seen in Fig. 2. The identification of the microscopic mechanism seems, however, to be hard to make. The linear dependence of the critical stress evidenced by Eq. (3), seems to agree with a thermal activation mechanism, as given by Eq. (2), and an analogy with a dislocation moving in a cloud of point defects,²⁸ but the frequency dependence predicted by such a model has been impossible to detect by changing the frequency in a wide range in our pendulum.²⁹ The evidence is thus ambiguous, with the frequency independence arguing against a simple mechanism of thermal activation, and the stress dependence being atypical of a true phase transition. It should be remembered that both interpretations are rather drastic simplifications of the physical situation, which is much more complicated, since one has an elastic lattice interacting with pinning centers which presumably have a broad spectrum of energies. Perhaps the relevant model should have to be changed, and it would perhaps be worthwhile to explore the recently proposed idea of self-organized criticality³⁰ (SOC) in the context of FLL dynamics. Some of the models proposed for study in SOC, such as that for earthquakes,³¹ seem to be appropriate for being translated for FLL problems. The fact that $1/f$ noise has been observed in the FLL (32) is another piece of corroborating evidence, although more work is clearly necessary to establish the worth of this hypothesis.

ACKNOWLEDGMENTS

We gratefully acknowledge fruitful discussions with G. D'Anna, G. Gremaud, L. Forro, and A. Kulik and M. Longchamp and G. D'Anna for technical assistance.

*Permanent address: Centro Atómico, (8400) Bariloche, Argentina.

¹E. H. Brandt, P. Esquinazi, and H. Neckel, *J. Low Temp. Phys.* **63**, 187 (1986), P. Esquinazi, H. Neckel, G. Weiss, and E. H. Brandt, *J. Low Temp. Phys.* **64**, 1 (1986).

²P. L. Gammel, L. F. Schneemeyer, J. V. Wasczak, and D. J. Bishop, *Phys. Rev. Lett.* **61**, 1666 (1988).

³D. J. Baar and J. P. Harrison, *Physica C* **157**, 215 (1989).

⁴D. J. Baar, J. P. Franck, J. P. Harrison, Y. Lacroix, and M. K. Yu, *Physica C* **170**, 233 (1990).

⁵S. Gregory, C. T. Rogers, T. Venkatesan, X. D. Wu, A. Inam, and B. Dutta, *Phys. Rev. Lett.* **62**, 1548 (1989).

⁶H. Safar, C. Durán, J. Guimpel, L. Civale, J. Luzuriaga, E. Rodríguez, F. de la Cruz, C. Fainstein, L. F. Schneemeyer, and J. V. Wasczak, *Phys. Rev. B* **40**, 7380 (1989).

⁷E. Rodríguez, C. Durán, J. Luzuriaga, F. de la Cruz, and

- C. Fainstein, *Physica C* **165**, 315 (1990).
- ⁸E. Rodríguez, J. Luzuriaga, C. A. D'Ovidio, and D.A. Esparza, *Phys. Rev. B* **42**, 10 796 (1990).
- ⁹A. Gupta, P. Esquinazi, H. F. Braun, W. Gerhäuser, N. H. Neumüller, K. Heine, and J. Tenbrink, *Europhys. Lett.* **10**, 663 (1989).
- ¹⁰A. Gupta, P. Esquinazi, H. F. Braun, and N. H. Neumüller, *Phys. Rev. Lett.* **63**, 1869 (1989).
- ¹¹S. de Brion, R. Calemczuk, and J. Y. Henry, *Physica C* **178**, 225 (1991).
- ¹²M. J. Higgins, D. P. Goshorn, S. Bhattacharya, and D. C. Johnston, *Phys. Rev. B* **40**, 9393 (1989).
- ¹³J. Pankert, G. Marbach, C. Conberg, P. Lemmens, P. Fröning, and S. Ewert, *Phys. Rev. Lett.* **65**, 3052 (1990); J. Pankert, *Physica C* **168**, 335 (1990).
- ¹⁴Y. Horie, T. Miyazaki, and T. Fukami, *Physica C* **175**, 93 (1991).
- ¹⁵G. D'Anna, W. Benoit, J. Luzuriaga, and H. Berger, *Europhys. Lett.* **13**, 464 (1990).
- ¹⁶G. D'Anna, W. Benoit, and H. Berger, *Phys. Status Solidi A* **125**, 589 (1991).
- ¹⁷G. D'Anna and W. Benoit, *Rev. Sci. Instrum.* **61**, 3821 (1990).
- ¹⁸D. E. Farrell, J. P. Rice, and D. M. Ginsberg, *Phys. Rev. Lett.* **67**, 1165 (1991).
- ¹⁹D. R. Nelson, *Phys. Rev. Lett.* **60**, 1973 (1988); D. R. Nelson and S. Sebastian Seung, *Phys. Rev. B* **39**, 9153 (1989).
- ²⁰D. S. Fisher, M. P. Fisher, and D. A. Huse, *Phys. Rev. B* **43**, 130 (1991).
- ²¹M. P. A. Fisher, *Phys. Rev. Lett.* **62**, 1415 (1989).
- ²²R. S. Markiewicz, *J. Phys. C* **21**, L1173 (1988).
- ²³E. H. Brandt, *Z. Phys. B* **80**, 167 (1990).
- ²⁴Y. Yeshurun and A. P. Malozemoff, *Phys. Rev. Lett.* **60**, 2202 (1988).
- ²⁵M. Tinkham, *Phys. Rev. Lett.* **61**, 1658 (1988).
- ²⁶P. H. Kes, J. Aarts, J. van den Berg, C. J. van der Beek, and J. A. Mydosh, *Supercond. Sci. Technol.* **1**, 242 (1989).
- ²⁷A. S. Nowick and B. S. Berry, *Anelastic Relaxation in Crystalline Solids* (Academic, New York, 1972), p. 46.
- ²⁸G. Gremaud, *J. Phys. (Paris) Colloq.* **48**, C8-15 (1987).
- ²⁹J. Luzuriaga, M.-O. André, and W. Benoit (unpublished).
- ³⁰P. Bak, C. Tang, and K. Wiesenfeld, *Phys. Rev. Lett.* **59**, 381 (1987); *Phys. Rev. A* **38**, 364 (1988).
- ³¹P. Bak and C. Tang, *J. Geophys. Res.* **94**, 15 635 (1989).
- ³²G. J. van Gorp, *Phys. Rev.* **166**, 436 (1968).